Imaging Agents

Diketopyrrolopyrrole Bis-Phosphonate Conjugate: A New Fluorescent Probe for In Vitro Bone Imaging

Andrea Chiminazzo,[a] Giuseppe Borsato,[a] Alessia Favero,[b] Chiara Fabbro,[c] Charles E. McKenna,[d] Luca Giuseppe Dalle Carbonare,[e] Maria Teresa Valenti,[e] Fabrizio Fabris,[a] and Alessandro Scarso*[a]

Abstract: The synthesis of a conjugate molecule between an unusual red-fluorescent diketopyrrolopyrrole (DPP) unit and a bis-phosphonate (BP) precursor by a click-chemistry strategy to target bone tissue and monitor the interaction is reported. After thorough investigation, conjugation through a triazole unit between a γ-azido rather than a β-azido BP and an alkyne-functionalized DPP fluorophore group turned out to be the winning strategy. Visualization of the DPP-BP conjugate on osteoclasts and specific antiresorption activity were successfully demonstrated.

Introduction

Bis-phosphonates (BPs) are a family of compounds with structural similarity to pyrophosphate (Scheme 1 A), an important component of hydroxyapatite (HAP), the major constituent of the mineral portion of bones. This led to their extended use as specific bone-targeting drugs in the treatment of disorders of bone metabolism such as Paget's disease, hypercalcemia, and osteoporosis.[1] Bone matrix is constantly formed by osteoblasts and degraded by osteoclasts, and recent studies demonstrated the cellular activity of bis-phosphonates (BPs) acting as potent inhibitors of specific enzymes such as farnesyl diphosphate synthase (FDPS) and geranylgeranyl diphosphate synthase (GGPPS) in osteoclasts.[2,3] Zoledronic acid, an *N*-linked 1,3-diazole bis-phosphonate (Scheme 1 B) is among the most popular and efficient inhibitors of bone resorption targeting the above-mentioned enzymes identified to date. Commonly, BP drugs could be also used in the diagnosis of bone diseases,

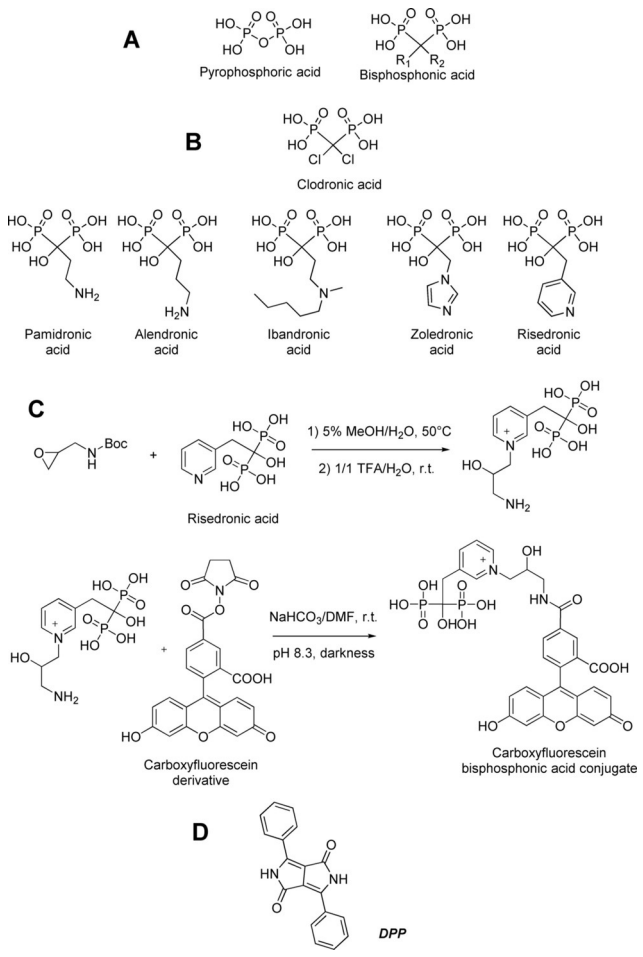

Scheme 1. A) Structures of pyrophosphoric acid and a general bis-phosphonic acid. B) Commercially available bis-phosphonic acids to contrast bone diseases. C) Examples of BP–fluorophore conjugates. D) Structure of 3,6-diphenyl-2,5-dihydropyrrolo[3,4-c]pyrrole-1,4-dione (DPP).

[a] *Dr. A. Chiminazzo, Dr. G. Borsato, Prof. Dr. F. Fabris, Prof. Dr. A. Scarso*
Dipartimento di Scienze Molecolari e Nanosistemi
Università Ca' Foscari di Venezia
via Torino 155, 30172 Mestre (VE) (Italy)
E-mail: alesca@unive.it

[b] *A. Favero*
Dipartimento di Scienze Chimiche della Vita e della Sostenibilità Ambientale, Università di Parma (Italy)

[c] *Dr. C. Fabbro*
Department of Chemistry, Imperial College London
Wood Lane, London W12 0BZ (UK)

[d] *Prof. Dr. C. E. McKenna*
Department of Chemistry, University of Southern California
Los Angeles, California 90089 (USA)

[e] *Prof. L. G. Dalle Carbonare, Prof. Dr. M. T. Valenti*
Dipartimento di Medicina, Università di
Verona (Italy)

Supporting information and the ORCID identification number(s) for the author(s) of this article can be found under:
https://doi.org/10.1002/chem.201805436.

in which, by means of appropriate linkers, they convey radioactive metals such as ^{99m}Tc[4,5] and ^{68}Ga to bones.[6]

Over the past two decades, optical imaging, including fluorescence, has become an attractive tool with unprecedented advantages in live-cell imaging, with the aim of examining and monitoring disease stages and determining therapy effectiveness in preclinical models both on cell cultures and on living tissues. In 2008 McKenna and collaborators were the first to report the synthesis of a fluorescent-labeled conjugate of a bis-phosphonic acid, specifically risedronate, using an epoxide linker strategy that enabled conjugation of BP with a carboxyfluorescein label (Scheme 1 C).[7] This strategy was extended to several BP–dye combinations[8] to create and test a toolkit of bone-imaging fluorescent probes with variable spectroscopic properties, bone-mineral binding affinities, and anti-prenylation activities.[9] Other fluorescent probes for bone imaging were developed by Kikuchi and collaborators,[10] who reported a pH-dependent BP–boron dipyrromethene probe for the detection of bone-resorbing osteoclasts and α-bis-substituted fluorescent BPs.[11] Near-infrared (NIR) fluorescence is also suitable for in vivo studies on bone minerals and cells, whereby the covalent conjugation of a BP to an NIR fluorophore created a highly potent bifunctional molecule for biomedical imaging.[12–14] Most of the BP fluorescent probes so far synthesized are based on well-known fluorophores such as Carboxyfluorescein (FAM), AlexaFluor 647 (AXF647), rhodamine red (RhR), and carboxyrhodamine (ROX).

Diketopyrrolopyrrole (DPP) is a fluorescent scaffold that is easily tunable in its absorption and emission properties and readily synthesized by reaction of an aromatic nitrile with a dialkyl succinate following a procedure developed by Ciba researchers (Scheme 1 D).[15] DPP has gained a pivotal role for the preparation of high-performance materials,[16] and important examples of its use as a reporting fluorescent unit to recognize biologically important species[17] have been reported to underline the potential of this chromophore as a fluorescent tag unit. DPP-based fluorescent probes for various other analytes, such as anions,[18] cations,[19] reactive oxygen species,[20] thiols,[21] pH,[22] CO_2,[23] and H_2,[24] are known. Fluorescent DPP derivatives as biological probes were reported by Bolze and collaborators,[25] who synthesized a DPP-based nonionic water-soluble two-photon-excited fluorescence (TPEF) microscopy dye characterized by high photostability, which was used in cofocal and TPEF microscopic evaluation of tumoral HeLa cell cultures. Structural modifications of the DPP unit have been carried out for the development of highly stable NIR dyes by Daltrozzo and collaborators,[26] also in the form of water-soluble NIR dyes.[27] Live-cell imaging showed easy internalization of these dyes into mammalian cells, and thus demonstrated their advantages for imaging applications and confirmed the intriguing properties of DPP-based dyes that make them new candidates for use as molecular probes in bio-imaging.

The bicyclic structure of DPP provides outstanding physicochemical stability and, in the visible region, shows an absorbance peak at 504 nm in solution and 538 nm in the solid state with high molar extinction coefficient (33850 L mol^{-1} cm^{-1}).[28] The Stokes shift ranging between 10 and 15 nm, the average fluorescence quantum yield of 60%, and its excellent photostability attracted the interest of several research groups in the chemical community because of its wide application as a fluorescent probe compared with other organic dyes. No fluorescent BP probes have been so far synthesized with DPP-based dyes as fluorophore group. The molecular framework of DPP has many reactive centers that undergo both electrophilic and nucleophilic reactions as well as different functional groups that may potentially undergo structural modification for further derivatization.[29]

Herein, we report on the synthesis of a bis-phosphonic acid–DPP conjugate (Scheme 2) obtained through a click reaction between an azido-BP and an alkyne-modified DPP and on the application of this conjugate fluorescent probe to bone tissue for imaging purposes. Conjugation by triazolinic bridge results in a new fluorescent probe in which antiresorption activity is maintained with the opportunity for use as a fluorescent probe for in vitro studies on osteoclast activity.

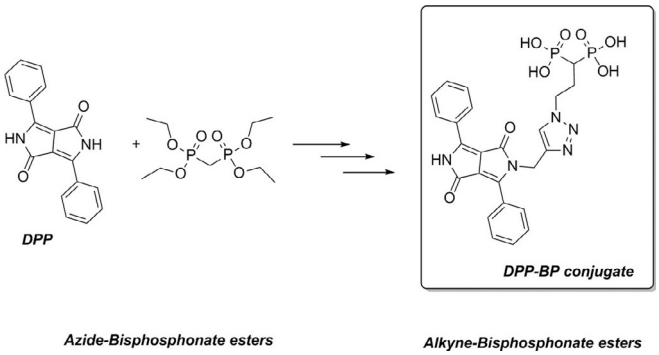

Scheme 2. Structure of the DPP–BP conjugate prepared and tested on bone tissue.

Results and Discussion

To conjugate the DPP fluorophore to a bis-phosphonate moiety, the click-chemistry copper(I)-catalyzed azide–alkyne cycloaddition (CuAAC) introduced by Sharpless et al. and Meldal et al.[30,31] was chosen. This is a virtually quantitative, very robust, general reaction, suitable even for biomolecular ligation,[32] that can be performed under a wide variety of conditions and with almost any source of solvated Cu^{I}.[33] $CuSO_4$ is usually used as catalyst with sodium ascorbate as reducing agent in water/*tert*-butanol (2:1) at room temperature under the conditions developed in the pioneering study by Sharpless and co-workers.

The conjugation between DPP and BP can be tackled by preparing an alkyne-substituted BP for reaction with an azide-derived DPP fluorophore or vice versa by preparing an azide-substituted BP for reaction with an alkyne DPP derived fluorophore (Scheme 3).

In the recent literature on BP synthesis, the first approach has been more extensively investigated owing to the straightforward preparation of tetraethyl(but-3-yne-1,1-diyl)bis-phosphonate (Scheme 3),[34] which has been exploited to bind

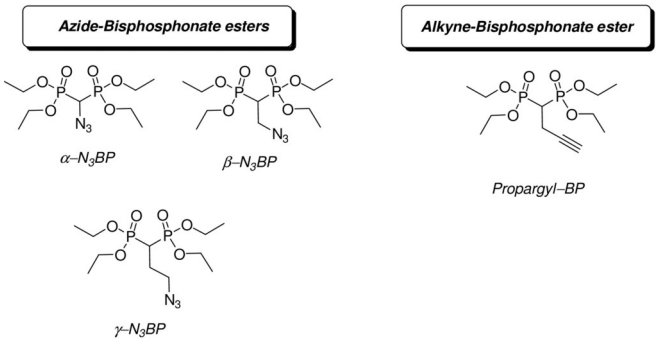

Scheme 3. Possible BP building block derivatives for click conjugation.

under click conditions, also with the aid of ultrasound,[35] to an anticancer pharmacophores,[36] and to a series of long hydrophobic tails to act as inhibitor of geranylgeranyl diphosphate synthase.[37,38,39,40] In one case, conjugation of the alkyne-BP with 3,5-bis(arylidene)-4-piperidinone units was accomplished to investigate potential antitumor properties.[36] A monopropargyl-substituted phosphonocarboxylate, structurally similar to BPs,[41] was reported to efficiently provide the corresponding triazole derivative.

At variance with the known literature, we decided to investigate the opposite approach consisting of the synthesis of an alkyne-substituted DPP fluorophore for click reaction with an azide-BP (Scheme 3).

Synthesis of alkyne-substituted DPP

Synthesis of the alkyne-substituted DPP started from the DPP core, which was prepared by following a literature procedure,[42] through protection of the N atoms with *tert*-butoxycarbonyl (Boc) groups to form the bis-Boc-DPP[43] (Scheme 4). The latter was monodeprotected by a newly optimized method consisting of the treatment of the bis-Boc-DPP reagent in CH_2Cl_2 with silica followed by solvent removal. The solid was then dried overnight under vacuum, loaded on a flash chromatography column, and isolated by using CH_2Cl_2/ethyl acetate (9/1) as eluent in satisfactory yield (62%). As we described previously,[44] the use of Boc protecting groups greatly enhances the solubility of the DPP pigment and enables the subsequent alkylation reaction with propargyl bromide[45] to give the final dissymmetric *tert*-butyl-1,4-dioxo-3,6-diphenyl-5-(prop-2-ynyl)-4,5-dihydropyrrolo[3,4-c]pyrrole-2(1*H*)-carboxylate (alkyneDPP-Boc) in an overall yield of 60% after column chromatography (Scheme 4).

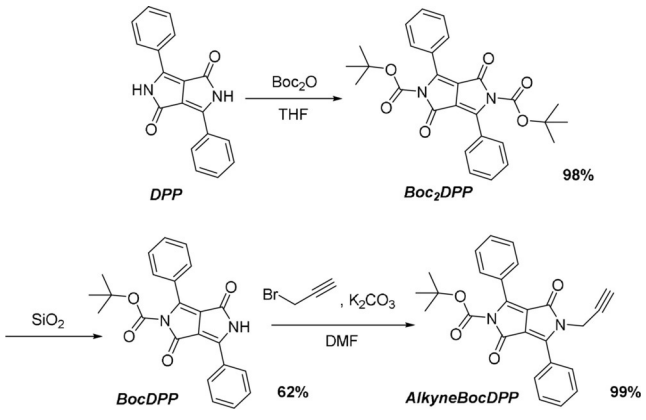

Scheme 4. Synthesis of AlkyneBocDPP from DPP by mono-deprotection followed by alkylation with propargyl bromide.

Synthesis of β-N_3 BP

As far as azide-containing BP precursors are concerned, only the synthesis of few examples of α-azido[46] and γ-azido BPs[47] have been described in the literature, but no click reactions have been reported for these compounds. Conversely, syntheses of and reactions with β-azido BP are highly discussed topics.[48,49] In particular, Chen and collaborators[48] published in 2013 the synthesis of tetraethyl 2-azidoethane-1,1-diyldiphosphonate (β-N_3BP) starting from vinylidene bis-phosphonate (VBP): the free azide product was obtained after only 15 min by reaction with sodium azide in water/acetic acid (1/1, *v*/*v*) at room temperature without formation of byproducts. On the contrary, in the same year Rodriguez and collaborators[50] showed that treating an excess of VBP with sodium azide in water at room temperature, did not lead to the direct formation of β-N_3BP (Scheme 5) but rather to the formation of

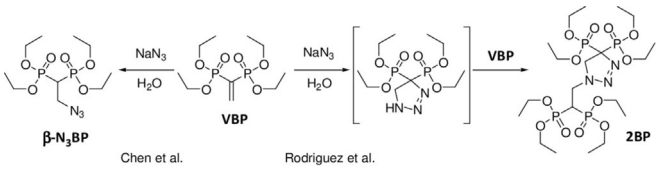

Scheme 5. Reported contrasting syntheses of β-azido bis-phosphonate.

double BP compound 2BP, likely because of the 1,3-dipolar cycloaddition leading to the triazole-BP intermediate. Once produced, the latter cyclic product reacted immediately with another molecule of VBP to undergo a Michael-type reaction yielding 2BP. NMR spectroscopic data supported this structure.

In this work, an alternative synthetic route is proposed for β-N_3BP that avoids the use of NaN_3 and working in organic medium to facilitate both the reactivity of hydrophobic substituted BP precursors and the isolation of the organic azide. Similarly to the previously reported metal-catalyzed addition of cyanide to BP precursors by using trimethylsilyl cyanide (TMSCN),[51] we investigated the azide addition reaction of trimethylsilyl azide ($TMSN_3$) to vinylidene bis-phosphonate tetraethyl ester to obtain β-azido BPs (Scheme 6) under different experimental conditions (Table 1).

The reaction was initially investigated with different metal precursors with 5 mol% catalyst loading. Cu^{II} and Zn^{II} did not lead to the formation of the desired product at room temperature (Table 1, entries 1 and 3). Whereas the Cu^{II} catalyst was inactive also under high-temperature conditions (Table 1, entry 2), Zn^{II} showed formation in moderate yield of the unex-

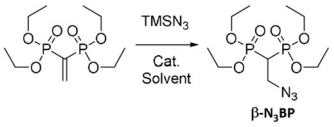

Scheme 6. Addition of $TMSN_3$ to VBP under different experimental conditions.

Table 1. Addition of $TMSN_3$ to VBP under different experimental conditions.[a]

Entry	BP	Catalyst	Solvent	*T* [°C]	Yield of azido BP [%][b]	Yield of amino BP [%][b]
1	VBP	$Cu(OTf)_2$	CH_2Cl_2	RT	0	0
2	VBP	$Cu(OTf)_2$	toluene	110	0	0
3	VBP	$Zn(OTf)_2$	CH_2Cl_2	RT	0	0
4	VBP	$Zn(OTf)_2$	toluene	110	0	20
5	VBP	$PdCl_2$	CH_2Cl_2	RT	>98 (26)[c]	0 (0)[c]
6	VBP	$Pd(OAc)_2$	CH_2Cl_2	RT	>98 (>98)[d]	0 (0)[d]
7	VBP	$Pd(OAc)_2$	toluene	110	0	90
8	VBP	$Pd(OAc)_2$	toluene	90	0	90
9	VBP	$Pd(OAc)_2$	toluene	60	15	75
10	VBP-Me	$Pd(OAc)_2$	CH_2Cl_2	RT	>98	0
11	VBP-Me	$Pd(OAc)_2$	toluene	110	0	90

[a] Reaction conditions: 0.07 mmol of VBP, 5 equiv $TMSN_3$, 5 mol% catalyst loading, 2 mL solvent, $t = 18$ h. [b] ^{31}P NMR yield. [c] 2 mol% catalyst loading. [d] 0.8 mmol of VBP.

pected product tetraethyl 2-aminoethene-1,1-diyldiphosphonate ($VBPNH_2$; Table 1, entry 4).

The use of Pd^{II} as metal catalyst (5 mol%) led to good activity, giving the desired tetraethyl 2-azidoethane-1,1-diyldiphosphonate (β-N_3BP) in excellent yields at room temperature, while decreasing the metal loading to 2 mol% resulted in only partial conversion (Table 1, entries 5 and 6). Pd^{II}-catalyzed addition of $TMSN_3$ to VBP under high temperature (Table 1, entry 7) did not lead to formation of β-N_3BP but provided the unsaturated $VBPNH_2$ in good yields (Scheme 7). Decreasing the reaction temperature to 60 °C led to the formation of both products (Table 1, entry 9). The formation of $VBPNH_2$ could probably be due to a thermal elimination of an N_2 molecule (Scheme 7).

Similarly, we investigated the same reaction with the vinylidene bis-phosphonate tetramethyl ester VBP-Me and observed both 2-azidoethane-1,1-diyl diphosphonate tetraethyl ester (β-N_3BP-Me) by Pd^{II}-catalyzed addition at RT (Table 1, entry 10) and tetramethyl 2-aminoethene-1,1-diyldiphosphonate ($VBPNH_2$-Me) on increasing the temperature to 110 °C (Table 1, entry 11). The resulting β-N_3BP was found to be stable for several days if stored at −20 °C, whereas decomposition and partial formation of 2BP were observed at room temperature. This phenomenon could be explained by assuming a retro-Michael reaction giving back some VBP, which can undergo a 1,3-cycloaddition with the remaining β-N_3BP leading to the formation of 2BP as byproduct, as in Scheme 5. Repeating the reaction with 0.8 mmol of VBP (Table 1, entry 6) showed that it can be easily scaled up without relevant loss of product yield. All the new azido and amino BP products were isolated and characterized by ^1H and ^{31}P NMR spectroscopy. Figure 1 shows the ^1H and $^{31}P\{^1H\}$ NMR spectra of VBP, β-N_3BP, and $VBPNH_2$, in which their typical ^1H and ^{31}P signals are present.

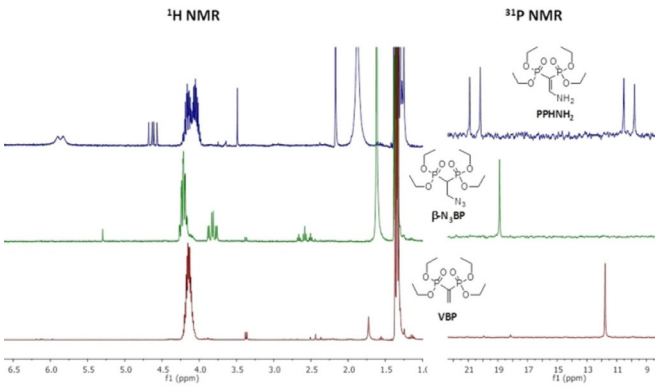

Figure 1. ^1H and $^{31}P\{^1H\}$ NMR spectra of VBP, β-N_3BP, and $VBPNH_2$.

To investigate the addition of $TMSN_3$ to substituted VBP precursors, optimized catalytic conditions were tested also with the substituted unsaturated BP precursor PPH (Scheme 8). Whereas Pd^{II} was an excellent metal catalyst in $TMSN_3$ addition to VBP, it was less reactive with respect to monosubstituted VBP precursors such as PPH (Table 2, entries 1–4). Increasing the catalyst amount to 10 mol% did not result in a substantial increase in reaction yields (Table 2, entries 2 and 3), even under drastic temperature conditions (Table 2, entries 4 and 5). The use of $Zn(OTf)_2$, which showed modest reactivity with VBP (Table 1, entry 4), led to the formation of the desired tetraethyl 2-azido-2-phenylethane-1,1-diyldiphosphonate (N_3PPH) in moderate yield (Table 2, entry 6). Increasing the temperature moderately increased the reaction yield (Table 2, entry 7) but at the same time led to predominant formation of tetraethyl 2-

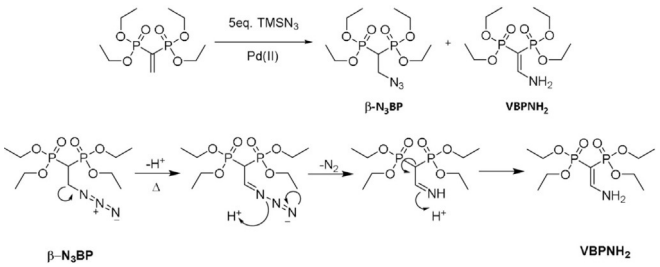

Scheme 7. Addition of $TMSN_3$ to VBP provides different nitrogen BP products depending on the reaction temperature, and proposed N_2 thermal elimination mechanism leading to$VBPNH_2$.

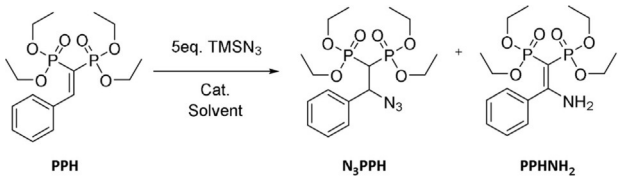

Scheme 8. Addition of $TMSN_3$ to PPH forming different nitrogen BP products depending on the reaction temperature.

Table 2. Addition of $TMSN_3$ to PPH under different experimental conditions.[a]

Entry	Catalyst	[Cat.] [mol%]	Solvent	T [°C]	Yield of azido BP[b] [%]	Yield of amino BP[b] [%]
1	$PdCl_2$	5	CH_2Cl_2	RT	5	0
2	$Pd(OAc)_2$	5	CH_2Cl_2	RT	5	0
3	$Pd(OAc)_2$	10	CH_2Cl_2	RT	7	0
4	$Pd(OAc)_2$	10	toluene	90	7	0
5	$Pd(OAc)_2$	10	toluene	110	10	0
6	$Zn(OTf)_2$	10	toluene	RT	30	0
7	$Zn(OTf)_2$	10	toluene	60	20	60
8	$Zn(OTf)_2$	10	toluene	90	0	90

[a] Reaction conditions: 0.07 mmol of PPH, $TMSN_3$ 5 equiv., 2 mL of solvent, $t = 18$ h. [b] ^{31}P NMR yield.

amino-2-phenylethene-1,1-diyldiphosphonate ($PPHNH_2$). Further increase of the reaction temperature led only to the formation of $PPHNH_2$ (Table 2, entry 8).

Despite numerous purification attempts, it was not possible to isolate N_3PPH as a pure product. Reduction of the azido moiety as well as functionalization of other substituted VBP precursors will be the subject of future studies to obtain a new class of β-amino BPs or β-azido BPs for further functionalization.

After optimization of the synthesis of β-azido BP we investigated its reaction with an fluorescent alkynyl DPP derivative using CuAAC (Scheme 9). Under the reaction conditions reported by Sharpless and co-workers,[30] the CuAAC was first attempted between β-N_3BP and AlkyneBocDPP as terminal alkyne (Scheme 9). The use of $CuSO_4$/ascorbic acid (1/2 molar ratio) catalyst and water/*tert*-butanol as solvent resulted in degradation of the azido BP, forming basically the starting VBP reagent. Even with the methyl-ester-protected azido-BP, the reaction did not work properly, and only VBP-Me was recovered as the main degradation product. Several attempts were made to prepare β-N_3BP in situ by adopting the reaction conditions reported by Chen and collaborators[48] starting from VBP and an excess of NaN_3. Unfortunately, no formation of azido BP occurred despite changing the solvent mixture or sonication, and only partial formation of triazolinic DPPBoc byproduct as consequence of the CuAAC reaction between NaN_3 and DPPBoc was observed. The CuAAC was tested between β-N_3BP and 1-octyne characterized by reduced steric hindrance with respect to DPPBoc but also in this case decomposition of the azido reagent occurred.

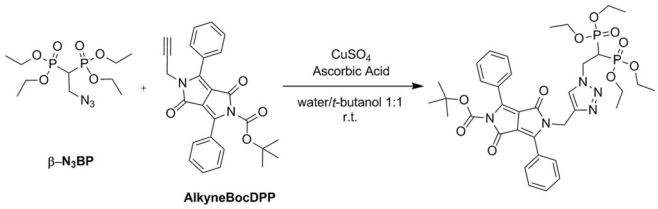

Scheme 9. CuAAC reaction between β-N_3BP and AlkyneBocDPP.

DPPBoc was tested in CuAAC under different reaction conditions with β-N_3BP as well as with VBP with an excess of NaN_3. The desired product was not obtained in any of the tested reactions reported, and only unchanged DPP and VBP were recovered. Even a preformed Cu^I catalyst such as chloro[1,3-bis(2,6-diisopropylphenyl)imidazol-2-ylidene]copper(I), known to be very active for CuAAC reactions[52,53] in very small catalytic amount,[54] failed to provide the expected product when used in an amount of 0.5 mol% in the reaction between β-N_3BP-Me and DPPBoc. Overall, the main problem that was observed is the instability of β-N_3BP in the presence of Cu^I species leading to a retro-Michael addition forming the VBP substrate. Because of this we decided to overcome this limit by synthesis of a γ-N_3BP, which should not display the same side reaction.

γ-N_3BP click reaction

We investigated a simple, straightforward, and easily scaled up synthesis of a γ-N_3BP through diazo transfer to 3-aminopropane-1,1-bis-phosphonate tetraethyl ester (γ-NH_2BP) using imidazole-1-sulfonyl azide hydrochloride as a much safer diazo-transfer reagent compared to the more common triflyl azide.[55] The γ-NH_2BP was prepared by reaction of nitromethane with VBP in the presence of sodium methylate (Scheme 10A) giving the corresponding 3-nitropropane-1,1-bis-phosphonate tetraethyl ester (γ-NO_2BP) in high yield on a multigram scale when a large excess of nitroalkane was used, in agreement with what was reported by Winckler and collaborators.[56] The catalytic hydrogenation of the nitro group of γ-NO_2BP was carried out at room temperature with 1 bar of hydrogen and Pd/charcoal under vigorous stirring to give the desired γ-NH_2BP in high yield (Scheme 10B). The hydrogenation was sensitive to the reaction time, and on prolonging the reaction to more than 1 h, the formation of several byproducts, probably due to dimerization or dealkylation of the ester moiety, was observed. Through this easy two-step route, the synthesis of γ-NH_2BP was accomplished on a multigram scale without the need for any purification step, but the product turned out to be quite

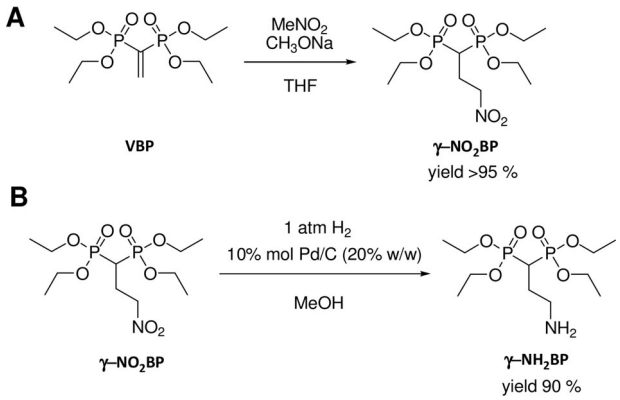

Scheme 10. Addition of nitromethane to VBP (A) and catalytic hydrogenation of γ-NO_2BP (B) forming γ-NH_2BP in high yield.

susceptible to decomposition; therefore, it could not be stored, and it was used right after preparation for the next diazo-transfer reaction.

Diazo-transfer reactions are commonly used for the introduction of diazo functionality or for converting primary amines to azides.[57,58,59] Zaloom and Roberts showed that triflyl azide (TfN_3) is excellent for converting α-amino acids to the corresponding α-azido acids.[60] The method was improved by Alper and collaborators,[61] who developed a $CuSO_4$-catalyzed version of the reaction. In the past decades, TfN_3 has been the reagent of choice for diazo-transfer reactions even though its standard synthetic protocol[62] has several disadvantages, such as the use of toxic and costly triflic anhydride, the use of an excess of sodium azide, and the formation of highly explosive TfN_3, which under no circumstances should be isolated. Recent advances in the field led to the introduction of a series of new safer and economic diazo-transfer reagents (Scheme 11).[55]

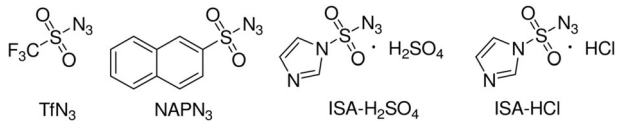

Scheme 11. Structures of common sulfonyl azides.

Imidazole-1-sulfonyl azide hydrochloride (ISA-HCl) was chosen as a safe and economical diazo-transfer reagent[64] to obtain the desired γ-N_3BP. This diazo donor was easily prepared by the addition of two equivalents of imidazole to chlorosulfonyl azide, preformed in situ by reaction of equimolar amounts of sodium azide and sulfuryl chloride in acetonitrile.[63] This one-pot reaction on a large scale allowed the synthesis of shelf-stable crystalline ISA-HCl from inexpensive materials (see Supporting Information). Attempts to synthesize a more stable and safer diazo donor such as imidazole-1-sulfonyl azide hydrogen sulfate (ISA-H_2SO_4)[64] resulted in an impractical viscous oil otherwise previously reported.

The diazo-transfer reaction between primary amino groups and organic azides can be efficiently catalyzed by $CuSO_4$,[61] and this class of catalytic reactions tolerates the presence of water well.[57] The reaction between γ-NH_2BP and ISA-HCl was carried out under mild basic conditions (aq. K_2CO_3, pH 8–10) at room temperature in the presence of 15 mol% of $CuSO_4$ (Scheme 12) to give a nearly quantitative yield of the desired γ-N_3BP.

Conversely, the use of the much safer diazo donor 2-naphthalenesulfonyl azide ($NAPN_3$)[65] resulted only in decomposition of the starting reagents. The synthesis of γ-N_3BP could be

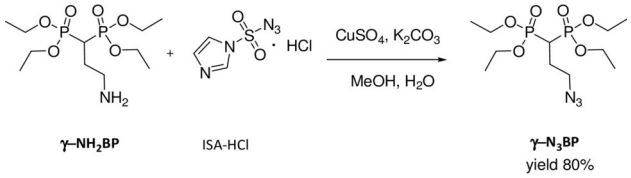

Scheme 12. Synthesis of γ-N_3BP by diazo transfer to γ-NH_2BP.

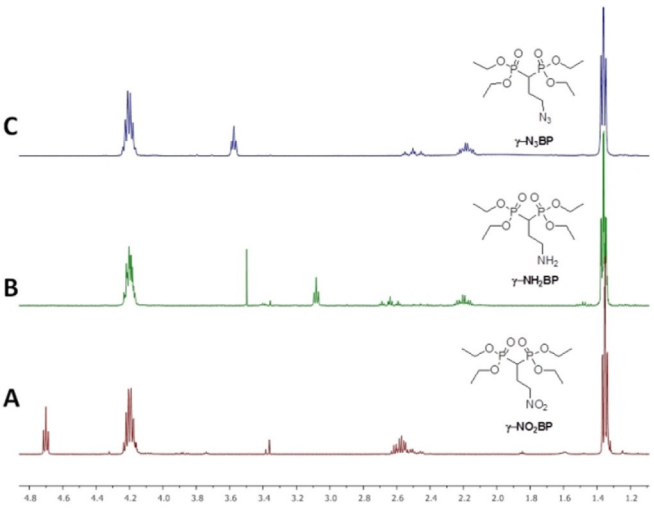

Figure 2. ^{1}H NMR spectra of A) γ-NO_2BP, B) γ-NH_2BP, and C) γ-N_3BP in $CDCl_3$.

scaled up to hundreds of milligrams without significant side effects. The γ-azido BP tetraethyl ester obtained was purified and characterized by ^{1}H and ^{31}P NMR spectroscopy like the other γ-BP compounds. Typical signals are reported in Figure 2.

The obtained γ-N_3BP was tested initially in the CuAAC click reaction with 3-butyn-1-ol as terminal alkyne due to its intrinsic low alkyne reactivity, which could mimic the behavior of the DPP fluorophores (Scheme 13, Table 3).

The use of 5 mol% $CuSO_4$ catalyst with 10 mol% ascorbic acid did not promote the click reaction (Table 3, entry 1). Changing the solvent mixture and the use of an equimolar amount of copper catalyst led to moderate yields of the desired cycloaddition product tetraethyl 3-(4-(2-hydroxyethyl)-1*H*-

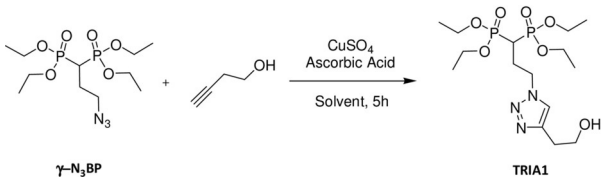

Scheme 13. CuAAC reaction between γ-N_3BP and 3-butyn-1-ol.

Table 3. Optimization of the CuAAC reaction conditions between γ-N_3BP and 3-butyn-1-ol.[a]

Entry	Alkyne [equiv]	Catalyst	Solvent	*T* [°C]	Yield[b] [%]
1	2	5 mol% $CuSO_4$ 10 mol% ascorbic acid	water/*t*BuOH (2:1)	RT	0
2	2	100 mol% $CuSO_4$ 200 mol% ascorbic acid	water/*i*PrOH (1:1)	RT	10
3	2	100 mol% $CuSO_4$ 200 mol% ascorbic acid	water/*i*PrOH (1:1)	50	78 75[c]
4	1.1	100 mol% $CuSO_4$ 200 mol% ascorbic acid	water/*i*PrOH (1:1)	50	70[c]

[a] Reaction conditions: 0.055 mmol of γ-N_3BP, 2 mL of solvent, 5 h. [b] ^{31}P NMR yield. [c] 2 h.

1,2,3-triazol-1-yl)propane-1,1-diyldiphosphonate (TRIA1, Table 3, entry 2). The reaction was influenced by the temperature, and it led to good yields of the desired product when carried out at 50 °C even after only 2 h (Table 3, entry 3). The reaction resulted in the formation of the 1,4-disubstituted cyclic adduct, as evidenced by ^{1}H NMR analysis. Good reaction yields and total γ-N_3BP consumption were also obtained on reducing the amount of the alkyne reagent (Table 3, entry 4). It is noteworthy that the yield of isolated triazole was moderate (26%). The hydroxyl group present in 3-butyn-1-ol enhances its hydrophilicity and thus makes isolation by organic-solvent extraction and purification difficult.

The optimized experimental conditions reported above were applied to the click reaction between γ-N_3BP and alkynyl-DPP-based fluorophore AlkyneBocDPP (Scheme 14). At variance with β-N_3BP, the click reaction between γ-N_3BP and AlkyneBocDPP occurred at the first attempt to give the corresponding desired 1,4-substituted triazolic cycloadduct (TRIA2) in 85% yield, without any difficulties, even in the extraction step from the aqueous solvent.

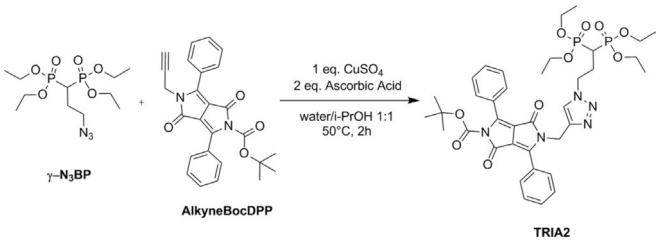

Scheme 14. CuAAC reaction between γ-N_3BP and AlkyneBocDPP.

The click reaction with AlkyneBocDPP was repeated on a ten times larger scale with 120 mg of γ-N_3BP, which allowed TRIA2 to be obtained in 90% yield without undesired byproducts. Purification by semi-automated column chromatography led to partial loss of a *tert*-butyloxycarbonyl group with consequent deprotection of the amino group of TRIA2, as demonstrated by the splitting of the ^{1}H NMR signals (see Supporting Information) and confirmed by ESI-MS analysis. The singlet at 7.75 ppm assigned to the triazolic proton is in agreement with the literature[35,37] and thus confirms the exclusive formation of a 1,4-substituted triazolic ring. The partial loss of the Boc protecting group was not a problem, since the subsequent step was the removal of all protecting groups on the amino and phosphonate moieties. TRIA2 was subjected to deprotection of the ethyl ester groups, and the classical method[66] that makes use of TMSBr at room temperature in dichloromethane was compared to a microwave-assisted method in acetonitrile. The latter turned out to be considerably faster and allowed formation of the intermediate silyl ester in only 20 min reaction with 16 equiv of TMSBr at 1200 W power (Scheme 15).

The ^{31}P NMR analyses in [D_6]DMSO of TRIA2 deprotected by the classical method showed formation of numerous signals, due both to partial deprotection of the ethyl ester groups and to decomposition of the molecule. In contrast, ^{31}P NMR analyses in [D_6]DMSO of TRIA2 deprotected by the microwave-assisted method showed the formation of only a sharp signal that was attributed to the corresponding 3-(4-{[1,4-dioxo-3,6-diphenyl-4,5-dihydropyrrolo(3,4-c)pyrrol-2(1*H*)-yl]methyl}-1*H*-1,2,3-triazol-1-yl)propane-1,1-diyldiphosphonic acid (FLUOProbe). The ^{1}H NMR spectrum (Figure 3) of TRIA2 demonstrated that this method ensured also the complete loss of the *tert*-butoxycarbonyl group to give FLUOProbe in its final structure, to be tested as a potential fluorescent probe for in vitro studies on osteoclast activity.

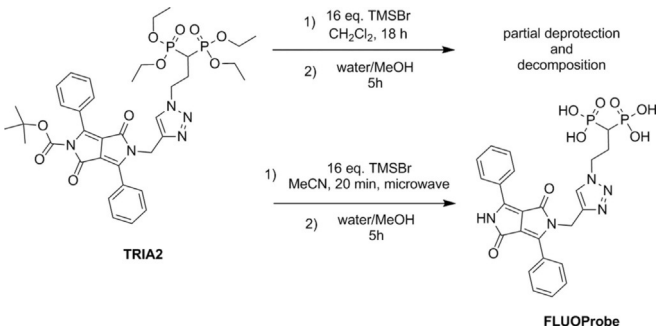

Scheme 15. Classic and microwaves assisted deprotection methods for the synthesis of FLUOProbe.

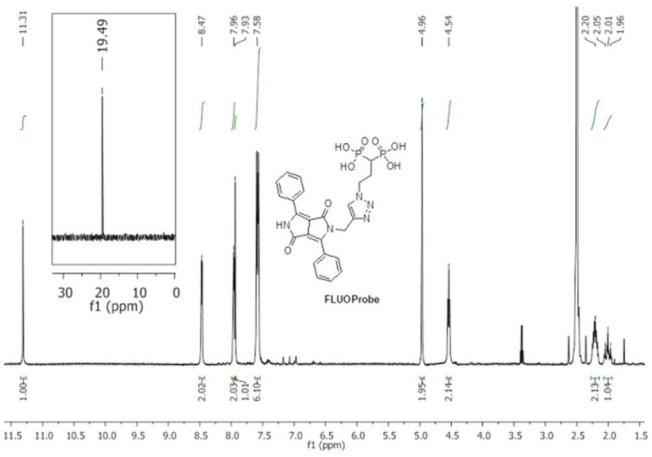

Figure 3. ^{1}H and ^{31}P{^{1}H} NMR spectra of FLUOProbe in [D_6]DMSO.

FLUOProbe was washed with diethyl ether to remove HBr formed as byproduct in the deprotection step and fully characterized by NMR spectroscopy and ESI-MS. Elemental analysis confirmed good purity (85%) and the product was further used for spectroscopic analysis, fluorescence tests, and biological activity studies.

Spectroscopic characterization of FLOUProbe

The UV/Vis spectrum of a solution of FLUOProbe in water/DMSO showed an intense absorption at 472 nm. Fluorescence analysis of the same solution showed an emission at 512 nm,

that is, a Stokes shift of 40 nm, which is much larger than the typical average value of 10–15 nm for the original DPP scaffolds (Figure 4).

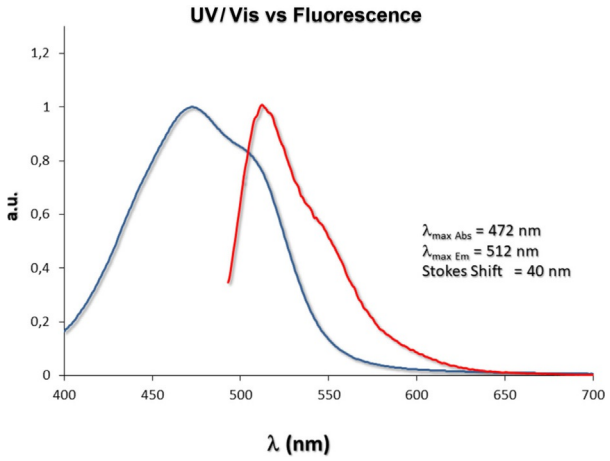

Figure 4. UV/Vis and fluorescence spectra of a solution of FLUOProbe in water/DMSO.

The method based on UV turbidity detection popularized by Lipinski and others[67] was chosen to determine the solubility of FLUOProbe. This method, albeit characterized by some limitations,[68] provided us with a rough estimation of the solubility of FLUOProbe, which is fundamental information for designing subsequent in vitro studies. UV absorbance was measured at 620 nm, a wavelength at which FLUOProbe showed very low absorbance, and the measurement was repeated for several solutions in a wide range of concentrations.[69] Precipitation was observed, as confirmed by an increase in absorbance due to light scattering owing to the formation of particulate material. The precipitation range was calculated from a plot of absorbance versus FLUOProbe concentration (see Supporting Information). With 5 vol% DMSO, the solutions remained homogeneous up to 50 μM, whereas for a solution with 1 wt% DMSO, the maximum solubility was calculated to be lower than 2 μM, and this solvent composition was used since it is biocompatible with the activity tests.

Imaging and biological tests of FLUOProbe on bone

FLUOProbe was used for a series of in vitro tests to investigate its affinity for bone matrix. A solution of FLUOProbe in α-MEM (Life Technologies) was added to bovine cortical bone slice. Microscopic (fluorescence) analyses demonstrated that the synthesized BP probe bearing the DPP fluorophore was able to bind efficiently to hydroxyapatite to result in a reddish material (Figure 5 and inset). This indicates that these cells can take up FLUOProbe and thus become clearly fluorescent and easily recognizable and localizable.

The osteoclast resorption activity was assayed by plating the cells (cultured with α-MEM by Life Technologies) supplemented with 10% fetal bovine serum (FBS) and in the presence of 25 ng mL^{-1} recombinant human macrophage colony stimulating factor (rh-MCSF) plus 30 ng mL^{-1} rh-RANKL (R&D Systems) on untreated and FLUOProbe-treated hydroxyapatite. Whereas on pure hydroxyapatite resorbance lacunae were present (Figure 6A), no osteoclast activity was found on treated HAP (Figure 6B), and this suggests that FLUOProbe shows potentially antiresorptive properties. Further analyses will be performed to assess the cytotoxicity of the synthesized fluorescent probe as well as anabolic ability by treating mesenchymal stem cells during osteogenic commitment.

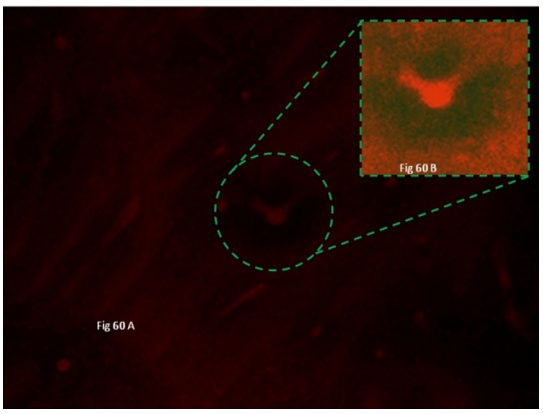

Figure 5. Fluorescence microscopy of FLUOProbe-treated bovine cortical bone.

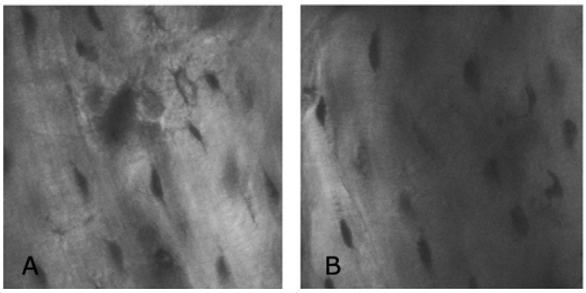

Figure 6. Osteoclast resorbing activity tests. Untreated (A) and FLUOProbe-treated (B) HAP.

Conclusion

We have reported the synthesis of a conjugate between an unusual red-fluorescent DPP unit and a BP precursor to provide a new tool to target bone and monitor the interaction. After thorough investigation, conjugation through a triazole unit between γ-azido rather than β-azido BP and an alkyne-functionalized DPP fluorophore group was found to be successful. Visualization of the DPP-BP conjugate on osteoclasts and specific antiresorption activity were successfully demonstrated.

Acknowledgements

The authors gratefully acknowledge Università Ca' Foscari for support.

Conflict of interest

The authors declare no conflict of interest.

Keywords: click chemistry · fluorescent probes · imaging agents · nitrogen heterocycles · phosphonates

[1] R. G. G. Russell, *Bone* **2007**, *40*, S21 – S25.
[2] Y. Zhang, R. Cao, F. Yin, M. P. Hudock, R. Guo, K. Krysiak, S. Mukherjee, Y. Gao, H. Robinson, Y. Song, J. Hwan No; K. Bergan, A. Leon, L. Cass, A. Goddard, T. Chang, F. Lin, E. Van Beek, S. Papapoulos, A. Wang, T. Kubo, M. Ochi, D. Mukkamala, E. Oldfield, *J. Am. Chem. Soc.* **2009**, *131*, 5153; K. Bergan, A. Leon, L. Cass, A. Goddard, T. Chang, F. Lin, E. Van Beek, S. Papapoulos, A. Wang, T. Kubo, M. Ochi, D. Mukkamala, E. Oldfield, *J. Am. Chem. Soc.* **2009**, *131*, 5153.
[3] A. J. Wiemer, J. S. Yu, L. W. Shull, R. J. Barney, B. M. Wasko, K. M. Lamb, R. J. Hohl, D. F. Wiemer, *Bioorg. Med. Chem.* **2008**, *16*, 3652.
[4] K. Libson, E. Deutsch, B. L. Barnett, *J. Am. Chem. Soc.* **1980**, *102*, 2476 – 2478.
[5] L. Qiu, W. Cheng, J. Lin, S. Luo, L. Xue, J. Pan, *Molecules* **2011**, *16*, 6165 – 6178.
[6] M. Meckel, M. Fellner, N. Thieme, V. Kubicek, F. Rösch, *Nucl. Med. Biol.* **2013**, *40*, 823 – 830.
[7] B. A. Kashemirov, J. L. F. Bala, X. Chen, F. H. Ebetino, F. P. Coxon, C. E. McKenna, *Bioconjugate Chem.* **2008**, *19*, 2308 – 2310.
[8] S. Sun, K. M. Błażewska, B. A. Kashemirov, F. P. Coxon, M. J. Rogers, F. H. Ebetino, C. E. McKenna, *Phosphorus Sulfur Silicon Relat. Elem.* **2011**, *186*, 970 – 971.
[9] S. Sun, K. M. Błażewska, A. P. Kadina, B. A. Kashemirov, J. E. Dunford, F. H. Ebetino, C. E. McKenna, *Bioconjugate Chem.* **2016**, *27*, 329 – 340.
[10] T. Kowada, J. Kikuta, A. Kubo, S. Mizukami, K. Kikuchi, *J. Am. Chem. Soc.* **2011**, *133*, 17772 – 17776.
[11] J. Gao, J. Liu, Y. Qiu, X. Chu, Y. Qiao, D. Li, *Biochim. Biophys. Acta* **2013**, *1830*, 3635 – 3642.
[12] K. M. Kozloff, L. I. Volakis, J. C. Marini, M. S. Caird, *J. Bone Miner. Res.* **2010**, *25*, 1748 – 1758.
[13] H. Hyun, H. Wada, K. Bao, J. Gravier, Y. Yadav, H. S. Choi, *Angew. Chem. Int. Ed.* **2014**, *53*, 10668 – 10672; *Angew. Chem.* **2014**, *126*, 10844 – 10848.
[14] a) S. Rudnick-Glick, E. Corem-Salkmon, I. Grinberg, R. Yehuda, S. Margel, *J. Nanobiotechnol.* **2015**, *13*, 80; b) S. Rudnick-Glick, E. Corem-Salkmon, I. Grinberg, S. Margel, *J. Nanobiotechnol.* **2016**, *14*, 80; c) N. Tal, S. Rudnick-Glick, S. Margel, *Polymer* **2017**, *132*, 188 – 192.
[15] A. Iqbal, L. Cassar, Patent US4415685 A, **1983**.
[16] a) Y. Li, P. Sonar, L. Murphy, W. Hong, *Energy Environ. Sci.* **2013**, *6*, 1684 – 1710; b) C. B. Nielsen, M. Turbiez, I. McCulloch, *Adv. Mater.* **2013**, *25*, 1859 – 1880; c) D. Chandran, K. S. Lee, *Macromol. Res.* **2013**, *21*, 272 – 283.
[17] a) Y. Cao, Y. N. Wu, G. N. Wang, J. W. Yi, C. L. Yu, Y. X. Huang, L. G. Sun, Y. Bao, Y. X. Li, *J. Mater. Chem. B* **2017**, *5*, 5479 – 5487; b) P. Liang, Y. Wang, P. Wang, J. Zou, H. Xu, Y. Zhang, W. Si, X. Dong, *Nanoscale* **2017**, *9*, 18890 – 18896; c) Y. Cai, P. Liang, S. Li, B. Zhao, J. Shao, W. Huang, Y. Zhang, Q. Zhang, X. Dong, *Org. Chem. Front.* **2018**, *5*, 98 – 105; d) K. Shou, Y. Tang, H. Chen, S. Chen, L. Zhang, A. Zhang, Q. Fan, A. Yu, Z. Cheng, *Chem. Sci.* **2018**, *9*, 3105 – 3110.
[18] a) Y. Qu, J. Hua, H. Tian, *Org. Lett.* **2010**, *12*, 3320 – 3323; b) Y. H. Jeong, C. H. Lee, W. D. Jang, *Chem. Asian J.* **2012**, *7*, 1562 – 1566.
[19] a) G. Zhang, H. Li, S. Bi, L. Song, Y. Lu, L. Zhang, J. Yu, L. Wang, *Analyst* **2013**, *138*, 6163 – 6170; b) M. Kaur, D. H. Choi, *Sens. Actuators B* **2014**, *190*, 542 – 548.
[20] M. Kaur, D. S. Yang, K. Choi, M. J. Cho, D. H. Choi, *Dyes Pigm.* **2014**, *100*, 118 – 126.
[21] L. Deng, W. Wu, H. Guo, J. Zhao, S. Ji, X. Zhang, X. Yuan, C. Zhang, *J. Org. Chem.* **2011**, *76*, 9294 – 9304.
[22] T. Yamagata, J. Kuwabara, T. Kanbara, *Tetrahedron Lett.* **2010**, *51*, 1596 – 1599.
[23] S. Schutting, S. M. Borisov, I. Klimant, *Anal. Chem.* **2013**, *85*, 3271 – 3279.
[24] J. Mizuguchi, T. Imoda, H. Takahashi, H. Yamakami, *Dyes Pigm.* **2006**, *68*, 47 – 52.
[25] H. Ftouni, F. Bolze, J. F. Nicoud, *Dyes Pigm.* **2013**, *97*, 77 – 83.
[26] G. M. Fischer, A. P. Ehlers, A. Zumbusch, E. Daltrozzo, *Angew. Chem. Int. Ed.* **2007**, *46*, 3750 – 3753; *Angew. Chem.* **2007**, *119*, 3824 – 3827.
[27] S. Wiktorowski, C. Rosazza, M. J. Winterhalder, E. Daltrozzo, A. Zumbusch, *Chem. Commun.* **2014**, *50*, 4755 – 4758.
[28] S. Luňák Jr., J. Vyňuchal, R. Hrdina, *J. Mol. Struct.* **2009**, *919*, 239 – 245.
[29] a) M. Grzybowski, D. T. Gryko, *Adv. Opt. Mater.* **2015**, *3*, 280; b) M. Kaura, D. H. Choi, *Chem. Soc. Rev.* **2015**, *44*, 58 – 77.
[30] V. V. Rostovtsev, L. G. Green, V. V. Fokin, K. B. Sharpless, *Angew. Chem. Int. Ed.* **2002**, *41*, 2596 – 2599; *Angew. Chem.* **2002**, *114*, 2708 – 2711.
[31] C. W. Tornøe, C. Christensen, M. Meldal, *J. Org. Chem.* **2002**, *67*, 3057 – 3064.
[32] A. E. Speers, G. C. Adam, B. F. Cravatt, *J. Am. Chem. Soc.* **2003**, *125*, 4686 – 4687.
[33] H. Hagiwara, H. Sasaki, T. Hoshi, T. Suzuki, *Synlett* **2009**, *4*, 643 – 647.
[34] P. A. Turhanen, *J. Org. Chem.* **2014**, *79*, 6330 – 6335.
[35] S. Liu, W. Bi, X. Li, X. Chen, L. Qu, Y. Zhao, *Phosphorus, Sulfur Silicon Relat. Elem.* **2015**, *190*, 1735 – 1742.
[36] M. V. Makarov, E. Y. Rybalkina, Z. S. Klemenkova, G. V. Röschenthaler, *Russian Chem. Bull. Int. Ed.* **2014**, *63*, 2388 – 2394.
[37] V. S. Wills, C. Allen, S. A. Holstein, D. F. Wiemer, *ACS Med. Chem. Lett.* **2015**, *6*, 1195 – 1198.
[38] X. Zhou, S. V. Hartman, E. J. Born, J. P. Smits, S. A. Holstein, D. F. Wiemer, *Bioorg. Med. Chem. Lett.* **2013**, *23*, 764 – 766.
[39] R. A. Matthiesen, M. L. Varney, P. C. Xu, A. S. Rier, D. F. Wiemer, S. A. Holstein, *Bioorg. Med. Chem.* **2018**, *26*, 376 – 385.
[40] X. Zhou, S. D. Ferree, V. S. Wills, E. J. Born, H. Tong, D. F. Wiemer, S. A. Holstein, *Bioorg. Med. Chem.* **2014**, *22*, 2791 – 2798.
[41] O. I. Artyushin, S. N. Osipov, G. V. Röeschenthaler, I. L. Odinets, *Synthesis* **2009**, *21*, 3579 – 3588.
[42] a) A. Iqbal, M. Jost, R. Kirchmayr, J. Pfenninger, A. Rochat, O. Wallquist, *Bull. Soc. Chim. Belg.* **2010**, *97*, 615 – 643; b) A. C. Rochat, L. Cassar, A. Iqbal, EP0094911, **1983**.
[43] J. S. Zambounis, Z. Hao, A. Iqbal, EP0648770, **1995**.
[44] R. Beninatto, G. Borsato, O. De Lucchi, F. Fabris, V. Lucchini, E. Zendri, *Dyes Pigm.* **2013**, *96*, 679 – 685.
[45] a) G. Colonna, T. Pilati, F. Rusconi, G. Zecchi, *Dyes Pigm.* **2007**, *75*, 125 – 129; b) M. V. R. Raju, H.-C. Lin, *Org. Lett.* **2013**, *15*, 1274 – 1277; c) M. V. R. Raju, P. Raghunath, M. C. Lin, H. C. Lin, *Macromolecules* **2013**, *46*, 6731 – 6743.
[46] B. Chamberlain, T. Upton, B. Kashemirov, C. McKenna, *J. Org. Chem.* **2011**, *76*, 5132 – 5135.
[47] J. P. Gourves, H. Couthon, G. Sturtz, *Phosphorus Sulfur Silicon Relat. Elem.* **1998**, *132*, 219 – 229.
[48] X. Chen, X. Li, J. Yuan, L. Qu, S. Wang, H. Shi, Y. Tang, L. Duan, *Tetrahedron* **2013**, *69*, 4047 – 4052.
[49] M. Ferrer-Casal, A. P. Barboza, S. H. Szajnman, J. B. Rodriguez, *Synthesis* **2013**, *45*, 2397 – 2404.
[50] M. Ferrer-Casal, A. P. Barboza, S. H. Szajnman, J. B. Rodriguez, *Synthesis* **2013**, *45*, 2397 – 2404.
[51] A. Chiminazzo, M. Damuzzo, L. Sperni, G. Strukul, A. Scarso, *Helv. Chim. Acta* **2017**, *100*, e1700104.
[52] S. Díez-González, E. D. Stevens, S. P. Nolan, *Chem. Commun.* **2008**, 4747 – 4749.
[53] H. Díaz Velázquez, Y. Ruiz García, M. Vandichel, A. Madder, F. Verpoort, *Org. Biomol. Chem.* **2014**, *12*, 9350 – 9356.
[54] S. Díez-González, E. D. Stevens, S. P. Nolan, *Angew. Chem. Int. Ed.* **2008**, *47*, 8881 – 8884; *Angew. Chem.* **2008**, *120*, 9013 – 9016.
[55] H. Johansson, D. Pedersen, *Eur. J. Org. Chem.* **2012**, 4267 – 4281.
[56] W. Winckler, T. Pieper, B. Keppler, *Phosphorus Sulfur Silicon Relat. Elem.* **1996**, *112*, 137 – 141.
[57] R. Lartia, P. Murat, P. Dumy, E. Defrancq, *Org. Lett.* **2011**, *13*, 5672 – 5675.
[58] A. Mishra, V. K. Tiwari, *J. Org. Chem.* **2015**, *80*, 4869 – 4881.
[59] T. J. Sminia, D. S. Pedersen, *Synlett* **2012**, *23*, 2643 – 2646.
[60] J. Zaloom, D. Roberts, *J. Org. Chem.* **1981**, *46*, 5173 – 5176.
[61] P. Alper, S. Hung, C. Wong, *Tetrahedron Lett.* **1996**, *37*, 6029 – 6032.
[62] A. Link, M. Vink, D. Tirrell, *Nat. Protoc.* **2007**, *2*, 1879 – 1883.
[63] E. Goddard-Borger, R. Stick, *Org. Lett.* **2007**, *9*, 3797 – 3800.
[64] N. Fischer, E. Goddard-Borger, R. Greiner, T. Klapotke, B. Skelton, J. Stierstorfer, *J. Org. Chem.* **2012**, *77*, 1760 – 1764.
[65] A. Khare, C. E. Mckenna, *Synthesis* **1991**, *5*, 405 – 406.

[66] O. Bortolini, I. Mulani, A. De Nino, L. Maiuolo, M. Nardi, S. Avnet, *Tetrahedron* **2011**, *67*, 5635 – 5641.
[67] C. A. Lipinski, F. Lombardo, B. W. Dominy, P. J. Feeney, *Adv. Drug Delivery Rev.* **1997**, *23*, 3 – 25.
[68] A. Avdeef, B. Testa, *Cell. Mol. Life Sci.* **2002**, *59*, 1681 – 1689.
[69] C. A. Lipinski, F. Lombardo, B. W. Dominy, P. J. Feeney, *Adv. Drug Delivery Rev.* **2001**, *46*, 3 – 26.

Manuscript received: October 30, 2018
Accepted manuscript online: January 2, 2019
Version of record online: February 12, 2019